

Field Induced Orbital Antiferromagnetism in Mott Insulators

K. A. Al-Hassanieh,¹ C. D. Batista,¹ G. Ortiz,² and L. N. Bulaevskii¹

¹Theoretical Division, Los Alamos National Laboratory, Los Alamos, New Mexico 87545

²Department of Physics, Indiana University, Bloomington, IN 47405, USA

(Dated: August 30, 2021)

We report on a new electromagnetic phenomenon that emerges in Mott insulators, i.e., materials that do not conduct electricity because of strong electronic Coulomb repulsion. The phenomenon manifests as antiferromagnetic ordering due to orbital electric currents which are spontaneously generated from the coupling between spin currents and an external homogenous magnetic field. This novel spin-charge current effect provides the mechanism to detect the so far elusive spin currents by means of unpolarized neutron scattering, nuclear magnetic resonance or muon spectroscopy. We illustrate this mechanism by solving a half-filled Hubbard model on a frustrated ladder, a simple but nontrivial case of strongly interacting electrons.

PACS numbers: 72.80.Sk, 74.25.Ha, 73.22.Gk

Insulators are generically characterized by the presence of a gap to charge-carrying excitations, and classified according to the origin of this gap. The charge gap of Mott insulators is driven by intra-atomic electron-electron Coulomb interactions, and the half-filled Hubbard Hamiltonian is the minimal model that describes its properties. Mott insulators exhibit a very broad spectrum of physical properties due to the correlated nature of their electronic localization. While electrons are completely localized in the Wannier orbitals of band insulators, Mott insulators always exhibit a partial electronic delocalization due to the finitude of the Coulomb repulsion, U , relative to the kinetic energy or hopping amplitude t .

The combination of partial delocalization with the fermionic nature of electrons leads to the well known antiferromagnetic exchange, J , between localized spins \mathbf{S}_i . It was shown recently that this partial delocalization also leads to electronic charge redistribution for a subclass of bond-ordered spin states [1]. Even more surprisingly Mott insulators can also contain a distribution of orbital electric currents that emerge for chiral spin orderings [1]. These orbital currents are directly associated with the notion of scalar spin chirality [2, 3]

$$\chi_{jkl} = \mathbf{S}_j \times \mathbf{S}_k \cdot \mathbf{S}_l. \quad (1)$$

The main purpose of this Letter is to demonstrate that a uniform magnetic field can induce *orbital* antiferromagnetism, i.e., antiferromagnetic ordering due to orbital *electric* currents, by the stabilization of staggered spin currents and the subsequent interplay between these currents and the applied field. For this purpose we will consider a Hubbard Hamiltonian on a zig-zag chain (see Fig.1) with nearest-neighbor (next-nearest-neighbor) hopping amplitudes t_1 (t_2). The application of a magnetic field B increases the uniform magnetization along the field direction z . A spontaneous breaking of the remaining $U(1)$ symmetry of global spin rotation along the z -axis is prevented by quantum fluctuations (Mermin-Wagner theorem [4]). This implies the absence of usual magnetic ordering in the x - y plane: $\langle S_j^\eta \rangle = 0$ with $\eta = x, y$. We will show however that the so called “chiral spin orderings”, both vector chirality ($\langle \mathbf{S}_j \times \mathbf{S}_{j+1} \rangle \neq 0$) and scalar spin chirality

($\langle \chi_{ijk} \rangle \neq 0$), can be induced by the field. The field-induced vector chiral ordering is a remnant of the classical helical order $\langle S_j^\eta \rangle \neq 0$ that is obtained in the classical (large spin, $S \rightarrow \infty$) limit [5]. On the other hand, the scalar spin chirality results from the spontaneous vector spin chirality and the field induced magnetization, $\langle \chi_{jkl} \rangle \simeq \langle \mathbf{S}_j \times \mathbf{S}_k \rangle \cdot \langle \mathbf{S}_l \rangle$. As we will show below, this connection between scalar and vector spin chiralities implies a relation between electric and spin currents, i.e., a spin-charge current effect.

Chiral phases (nonzero scalar or vector spin chirality) in quantum spin chains were predicted a long time ago and have been studied for many years. As noted by Villain [6], the chiral ordering must survive at finite temperature (T) in weakly coupled chains, without the usual helical long-range ordering, since the chiral correlation length is much longer than the spin correlation length. In other words, there must be a window of temperatures where chiral order takes place in absence of helical order. There are experimental indications of the existence of such phase in the quasi-one dimensional organic magnet $\text{Gd}(\text{hfac})_3\text{NiTiPr}$ [5, 7]. However, the absence of external physical fields that couple to non-uniform chiral orderings poses a challenge for measuring these phases when there is no helical ordering [8]. *By showing that the field-induced vector chirality is accompanied by a staggered ordering of orbital magnetic moments (orbital electric currents), we provide a direct way of detecting this exotic phase by means of unpolarized neutron scattering, nuclear magnetic resonance (NMR) or muon spectroscopy (μ -SR).*

We start by considering a half-filled Hubbard model on the zigzag ladder with L sites ($0 \leq j \leq L-1$) depicted in Fig.1, and in the presence of magnetic field $\mathbf{B} = B\hat{z}$

$$H = \sum_{j,\nu,\sigma} (t_\nu c_{j\sigma}^\dagger c_{j+\nu\sigma} + \text{h.c.}) + \sum_j (U n_{j+} n_{j-} - B S_j^z), \quad (2)$$

where $\nu = 1, 2$, $\sigma = \pm 1$, $c_{j\sigma}^\dagger$ ($c_{j\sigma}$) creates (annihilates) an electron of spin σ at site j , $n_{j\sigma} = c_{j\sigma}^\dagger c_{j\sigma}$, $n_j = \sum_\sigma n_{j\sigma}$, and $S_j^\eta = \sum_{\alpha\beta} c_{j\alpha}^\dagger \sigma_{\alpha\beta}^\eta c_{j\beta} / 2$ are the spin-1/2 operators with σ^η the Pauli matrices. We assume periodic boundary conditions (PBC), i.e., $L \equiv 0$. In the large U/t_ν limit, the low-energy

spectrum of H is described by an effective Heisenberg spin-1/2 Hamiltonian,

$$\tilde{H} = \sum_{j,\nu} J_\nu (\mathbf{S}_j \cdot \mathbf{S}_{j+\nu} - \frac{1}{4}) - B \sum_j S_j^z, \quad (3)$$

because the electrons are localized near the lattice sites. \tilde{H} is obtained by projecting the original H into the low-energy subspace \mathcal{S} . This is true in general for any physical quantity, \mathcal{A} , whose effective low-energy operator, $\tilde{\mathcal{A}}$, is a function of the spin operators \mathbf{S}_j . The expression for $\tilde{\mathcal{A}}$ is obtained by a canonical transformation that follows from standard degenerate perturbation theory. The exchange constants are $J_\nu = 4t_\nu^2/U > 0$.

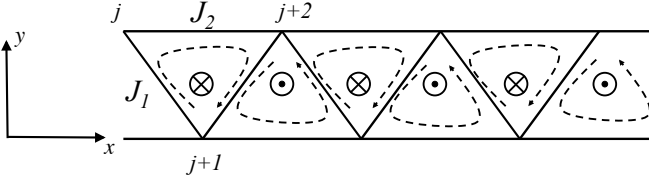


FIG. 1: Zigzag ladder. The arrows indicate the circulation of the spin and the electrical orbital currents that emerge in the ground state for $J_2 \gg J_1$ and $|B| \lesssim |B_{\text{sat}}|$, with B_{sat} the saturation field. The small circles indicate the orientation of the (staggered) magnetic moments generated by the electric currents.

We are interested in two physical quantities that will be particularly relevant for this work. These are the charge and the spin (z -component) current densities in a given bond $\langle jl \rangle$ (with $l = j + \nu$ and $t_{jl} = t_\nu$)

$$\begin{aligned} \mathbf{I}_{jl}^c &= i \sum_{\sigma} (c_{j\sigma}^\dagger c_{l\sigma} - c_{l\sigma}^\dagger c_{j\sigma}) \frac{et_{jl}}{\hbar} \hat{\mathbf{r}}_{jl}, \\ \mathbf{I}_{jl}^s &= i \sum_{\sigma} (c_{j\sigma}^\dagger c_{l\sigma} - c_{l\sigma}^\dagger c_{j\sigma}) \frac{\sigma t_{jl}}{\hbar} \hat{\mathbf{r}}_{jl}, \end{aligned} \quad (4)$$

where $\hat{\mathbf{r}}_{jl} = (\mathbf{r}_l - \mathbf{r}_j)/|\mathbf{r}_l - \mathbf{r}_j|$, and \mathbf{r}_j is the vector position of site j . Both are Noether currents for the charge and spin conservation laws associated with the corresponding U(1) and SU(2) global symmetries of H . The charge current has a non-zero low-energy effective operator, $\tilde{\mathbf{I}}_{jl}^c$, whenever the site j belongs to a loop that is closed by an odd number of hopping terms [1]. Since the shortest possible loop is a triangle, $\tilde{\mathbf{I}}_{jl}^c$ is $\mathcal{O}(t^{n+1}/U^n)$ with n odd and $n \geq 3$. Therefore, the lowest order contribution to the effective charge current density operator is [1]

$$\tilde{\mathbf{I}}_{jl}^c = \frac{24e}{\hbar} \hat{\mathbf{r}}_{jl} \sum_{l \neq j,k} \frac{t_{jl} t_{lk} t_{kj}}{U^2} \chi_{jkl}. \quad (5)$$

Equation (5) establishes a direct correspondence between the scalar chiral spin ordering, $\langle \chi_{ijk} \rangle \neq 0$, and the presence of electric orbital currents. In other words, most of the scalar spin orderings will be accompanied by the emergence of orbital currents. The effective spin current density operator is

$$\tilde{\mathbf{I}}_{jl}^s = \frac{8t_{jl}^2}{U} \kappa_{jl}^z \hat{\mathbf{r}}_{jl}, \quad \text{with } \kappa_{jl}^z = \mathbf{S}_j \times \mathbf{S}_l \cdot \hat{\mathbf{z}}. \quad (6)$$

This simple expression shows that the spin current is directly associated to the vector spin chirality. Since \mathbf{I}_{jl}^s is even under a particle-hole transformation ($t_{jl} \rightarrow -t_{jl}$, $\mathbf{S}_j \rightarrow -\mathbf{S}_j$), the prefactor on the right hand side of Eq. (6) can only contain even powers of the hopping amplitudes.

The effective current density operators introduced above are necessary to characterize the ground state correlations when the magnetic field approaches its saturation value B_{sat} , and $t_2 \gtrsim t_1$. As we will show below, this ground state exhibits long range order of spin and charge currents that are roughly proportional to each other when $J_2 \gg J_1$, and $|B| \lesssim |B_{\text{sat}}|$. To understand the origin of this instability, it is convenient to write \tilde{H} in terms of new fermionic degrees of freedom f_j by means of a Jordan-Wigner transformation

$$S_j^+ = f_j^\dagger K_j, \quad S_j^- = K_j f_j, \quad \bar{n}_j = S_j^z + \frac{1}{2}, \quad (7)$$

where $\bar{n}_j = f_j^\dagger f_j$ and $K_j = \prod_{k < j} (1 - 2\bar{n}_k)$ is the nonlocal operator that realizes the change in exchange statistics.

The new expression of \tilde{H} can be written as

$$\tilde{H} = \tilde{H}_1 + \tilde{H}_2 - B \sum_l \bar{n}_l, \quad (8)$$

$$\tilde{H}_1 = \frac{J_1}{2} \sum_l (f_l^\dagger f_{l+1} + f_{l+1}^\dagger f_l) + J_1 \sum_l (\bar{n}_l \bar{n}_{l+1} - \bar{n}_l)$$

$$\tilde{H}_2 = \frac{-J_2}{2} \sum_l (\kappa_l^z \kappa_{l+1}^z + \kappa_{l+1}^z \kappa_l^z) + J_2 \sum_l (\bar{n}_l \bar{n}_{l+2} - \bar{n}_l),$$

where $\kappa_l^z \equiv \kappa_{l+1}^z = i(f_l^\dagger f_{l+1} - f_{l+1}^\dagger f_l)$. Interestingly, we remark that the first term of \tilde{H}_2 is an explicit *ferromagnetic* interaction between spin currents on adjacent bonds. However, a state with net nearest-neighbors spin currents, $\langle \kappa_l^z \rangle \neq 0$, can only appear when $J_1 \neq 0$, i.e., for a finite coupling between upper and lower chains (see Fig.1).

To develop some intuition about the role played by J_1 , it is convenient to rewrite \tilde{H} in momentum space

$$\tilde{H} = \sum_k (\epsilon_k - \mu) a_k^\dagger a_k + \frac{1}{2L} \sum_{kpq} v_{pq} a_{q+p}^\dagger a_{k-p}^\dagger a_k a_q, \quad (9)$$

with $a_k^\dagger = \frac{1}{\sqrt{L}} \sum_{j=0}^{L-1} e^{ikj} f_j^\dagger$, $\epsilon_k = J_1 \cos k + J_2 \cos 2k$, $\mu = B + J_1 + J_2$, and $v_{pq} = 2\epsilon_p - 8J_2 \cos(p+2q)$. The first term is the non-interacting part of \tilde{H} , while the second contains the density-density interactions of \tilde{H}_1 and \tilde{H}_2 that lead to the first contribution, $2\epsilon_p$, plus a correlated second-nearest-neighbor hopping that is contained in the first term of \tilde{H}_1 , and leads to the second contribution in v_{pq} .

For $J_2 > J_1/4$, the fermion dispersion ϵ_k has two degenerate minima at $k = \pm Q$, with $\cos Q = -J_1/4J_2$, that correspond to opposite values of κ_l^z . The saturation field $B_{\text{sat}} = J_1 + J_2 - \epsilon_Q$ ($-B_{\text{sat}}$) corresponds to the critical value of the chemical potential at which the fermion density $\rho = \langle \bar{n}_j \rangle$ becomes equal to one (zero). From now on we will assume that the spin system is close to full polarization.

Since the physics is independent of the sign of B ($B \rightarrow -B$ under a time reversal transformation), we will choose the negative sign, $B \gtrsim -B_{\text{sat}}$, for the rest of the analysis. For the equivalent fermionic problem, this condition is equivalent to the dilute density limit, $\rho \ll 1$ or $\mu \gtrsim \epsilon_Q$.

For $J_1 = 0$, the symmetric and the anti-symmetric sectors generated by the fermionic operators $a_k^\dagger \pm a_{k+\pi}^\dagger$ are perfectly decoupled. In this case the spin currents are quenched since κ_l^z can only connect states on different sectors (it is odd under the transformation $k \rightarrow k + \pi$). The situation changes dramatically for $J_1/J_2 \ll 1$. At low energies, we can only have fermions a_k^\dagger near the two degenerate minima: $k \simeq \pm Q$. Since Q is close to $\pi/2$, the fermions $a_{\pm Q}^\dagger$ generate spin currents of nearly maximal amplitude and opposite signs: $\sum_l \kappa_l^z a_k^\dagger |0\rangle = \sin k a_k^\dagger |0\rangle$. While the non-interacting part of \tilde{H} favors a ground state in which both minima are equally populated (Pauli exclusion principle), the second term of v_{pq} leads to a nearest-neighbor attraction between fermions with the same chirality (in the same minimum) and a nearest-neighbor repulsion between fermions with opposite vector chiralities (different minima). This is also expected from the first term of \tilde{H}_1 and it implies the possibility of a chiral instability similar to the one originally proposed by Nersisyan and coauthors [9] for XY zig-zag spin chains (see also [10]). In fact, the chiral phase was recently found for $J_2 \gg J_1$ and $|B| \simeq B_{\text{sat}}$ [5] by using the mean-field decoupling of the bosonized version of \tilde{H} that was originally introduced in Ref. [9] for the anisotropic case. On the other hand, a straightforward mean-field approximation to Eq. (9) overestimates the stability of the chiral phase (it gives a wrong density dependence for the energy of the disordered state). Since mean-field approximations to interacting quasi-one-dimensional systems are always subjected to scrutiny, it is decisive to have a numerical confirmation of this phase. By using density-matrix renormalization group (DMRG), McCulloch and coauthors [11] recently found the chiral phase for $J_2 = J_1$, while Okunishi [12] reported a phase diagram that confirms the existence of a chiral phase for $J_2 \gg J_1$ and $|B| \simeq B_{\text{sat}}$.

We will now derive an important physical consequence of a chiral spin phase that was overlooked before. To simplify notation we introduce the definitions: $\chi_l \equiv \chi_{l+1l+2}$ and $\mathbf{I}_{l+1}^\gamma \equiv \mathbf{I}_l^\gamma$ with $\gamma = c, s$. The combination of a field induced magnetization, $m_z = \langle S_l^z \rangle$, and a net vector spin chirality $\langle \kappa_l^z \rangle \neq 0$ leads to a non-zero mean value of the *scalar spin chirality*

$$\chi_l \simeq m_z [\kappa_l^z + \kappa_{l+1}^z - \kappa_{l+2}^z]. \quad (10)$$

This simple expression shows that, to a good approximation, scalar and vector chiralities are proportional to each other, and the uniform magnetization m_z is the proportionality constant. This relationship attains a clear physical meaning when we look at Eqs. (5) and (6): the field induced vector chiral order contains orbital *electric currents* that are proportional to the

spin currents

$$\tilde{\mathbf{I}}_{jl}^c \simeq \frac{6e}{U} m_z \sum_{l \neq j, k} \left[\frac{t_{jl} t_{lk}}{t_{jk}} \tilde{\mathbf{I}}_{jk}^s + \frac{t_{jl} t_{jk}}{t_{kl}} \tilde{\mathbf{I}}_{kl}^s - \frac{t_{kl} t_{jk}}{t_{jl}} \tilde{\mathbf{I}}_{jl}^s \right]. \quad (11)$$

Figure 1 displays the circulation of electrical orbital currents (arrows) that are expected for the chiral-ordered ground state of the zig-zag chain ($J_2 \gg J_1$ and $|B| \lesssim |B_{\text{sat}}|$) according to Eq. (11). Remarkably, the application of a *uniform* magnetic field induces *orbital antiferromagnetism* via the (dominant) Zeeman coupling to the spin moments. The small circles in Fig. 1 indicate the orientation of the staggered orbital moments that these electric currents generate.

To test the validity of Eq. (11) we study the ground state properties of both H and \tilde{H} by means of the DMRG method [13]. We use PBCs [14] to eliminate spurious oscillations in the correlation functions due to boundary effects. The incommensurate nature of the ordered ground state makes the numerical calculation quite challenging [15]. In contrast to Ref. [12] we do not include any infinitesimal bias field and compute chiral-chiral correlators (instead of the order parameter $\langle \kappa_l \rangle$) to establish chiral long-range order. In the case of the Hubbard Hamiltonian H , we solve a chain of $L = 64$ sites for $t_2/t_1 = 1.6$, $U/t_1 = 20, 24$, and 30 . B is chosen such that $2m_z = 0.875$. The charge-current, $C^c(r) = \langle I_l^c I_{l+r}^c \rangle$, and the spin-current, $C^s(r) = \langle I_l^s I_{l+r}^s \rangle$, correlation functions are computed directly in the DMRG ground-state wave function.

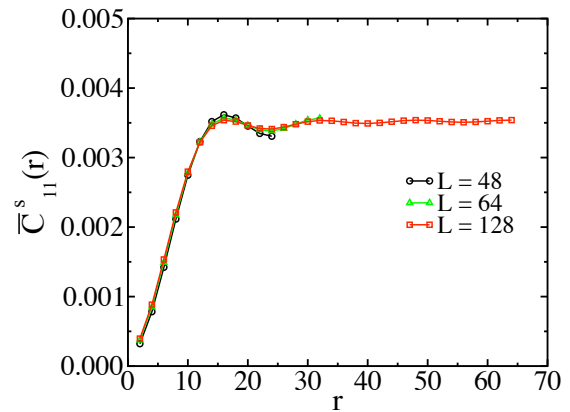


FIG. 2: Size dependence of the two-point vector spin chirality correlator $\tilde{C}_{nm}^s(r)$ for $J_2/J_1 = 2.56$ and $2m_z = 2\langle S_l^z \rangle = 0.875$.

For the Heisenberg model \tilde{H} , we study chains of lengths $L = 48, 64$, and 128 sites. The ratio between the exchange constants is determined by the ratio between the hopping amplitudes $J_2/J_1 = t_2^2/t_1^2 = 2.56$ and $2m_z = 0.875$. In this case we compute the vector spin chirality two-point correlation functions: $\tilde{C}_{nm}^s(r) = \langle \kappa_{l+n} \kappa_{l+r+l+m} \rangle$. Figure 2 shows $\tilde{C}_{11}^s(r)$ for different system sizes. The finite-size scaling clearly indicates the presence of long-range vector spin chiral order.

According to Eq. (6), the effective spin-current two-point correlation function is $C^s(r) = [8\frac{t_2^2}{U}]^2 \bar{C}_{11}^s(r)$. At long distances, the effective charge-current correlation function can be obtained approximately by using Eq. (10)

$$C^c(r) \simeq \tilde{\alpha} \langle \chi_l \chi_{l+r} \rangle \simeq 4\tilde{\alpha} m_z^2 [\bar{C}_{11}^s(r) - \bar{C}_{22}^s(r) + \frac{\bar{C}_{12}^s(r)}{4}],$$

with $\tilde{\alpha} = 2304t_1^4 t_2^2 / U^4$. Figures 3(a), (b) and (c) compares the spin-current two-point correlators computed with the Heisenberg (\tilde{H}) and the Hubbard (H) models for three different values of $U/t_1 = 20, 24$ and 30 .

As expected the results for the two models show better agreement as U increases. According to Eq. (12), the long-range ordered spin-currents (see Fig. 2) must lead to long-range ordered orbital electric currents. Figures 3(a), (b) and (c) show a comparison between $C^c(r) = \langle I_l^c I_{l+r}^c \rangle$ computed with the Hubbard Hamiltonian (H) for the same three different values of U , and the right-hand side of Eq. (12) computed with the Heisenberg model \tilde{H} . The good agreement between both curves confirms that the spin and the electric currents are approximately proportional to each other, with the proportionality constant linear in m_z . In other words, the ordering of spin currents is accompanied by ordering of orbital electric currents for non-zero m_z as follows from Eq. (10).

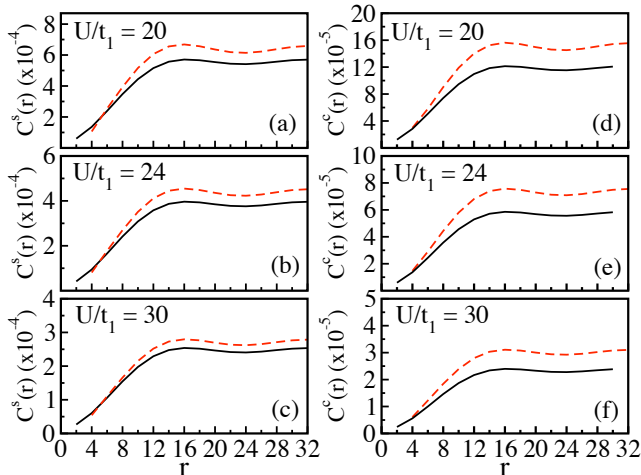


FIG. 3: (a), (b), (c) Charge-current correlation function $C^c(r)$ and (d), (e), (f) spin-current correlation function $C^s(r)$ in the case of the Hubbard model H (dashed lines) and the Heisenberg model \tilde{H} (solid lines). The results are shown for $L = 64$, $t_2/t_1 = 1.6$ ($J_2/J_1 = 2.56$), $\langle s_i^z \rangle = 0.4375$, and $U/t_1 = 20, 24$, and 30 .

The resulting staggered configuration of orbital magnetic moments implies that the ground state under consideration is a field-induced orbital antiferromagnet. We note that the orbital moments are located at the centers of the triangles (see Fig. 1), while the spin moments are obviously located at the corners (or sites of the lattice). The values of the orbital currents that we obtained for $U/t_1 = 20$ (see Fig. 3(d)) are of order $0.01 t_1$. The corresponding orbital magnetic moment is a few percent of a Bohr magneton for $t_1 \sim 1\text{eV}$. In contrast to the spin currents $\langle \kappa_l^z \rangle$, these orbital magnetic moments can be

measured with different experimental techniques such as neutron scattering, NMR or μ -SR. This provides a simple way of detecting this exotic spin ordering in real materials. Moreover, notice that the magnitude of the magnetic moment would be much larger if the chiral phase remains stable in the intermediate coupling regime $U \gtrsim t_\nu$.

To induce an electric current out of an spontaneously generated spin current (or vice-versa) one needs an externally applied magnetic field (or any other field that is odd under a time reversal transformation) since both currents have opposite parity under time reversal. This symmetry consideration has to be complemented by a microscopic mechanism that determines the magnitude of the spin-charge current conversion. The possibility of having orbital electric currents in frustrated Mott insulators [1] is the key for finding and quantifying such mechanism. This spin-charge current effect cannot be associated with a magnetoelectric response because the spin current does not couple directly to any electric or magnetic fields. On the other hand, the induced orbital electric currents can lead to small magnetoelectric effects. For instance, the application of an electric potential between the upper and lower chains (see Fig. 1) will lead to a net orbital magnetization because the magnetic moments in the lower and upper triangles will not be compensated any longer.

This work was carried out under the auspices of the National Nuclear Security Administration of the U.S. Department of Energy at Los Alamos National Laboratory under Contract No. DE-AC52-06NA25396.

-
- [1] L. N. Bulaevskii, C. D. Batista, M. Mostovoy, and D. Khomskii, *Phys. Rev. B* **78**, 024402 (2008).
 - [2] X. G. Wen, F. Wilczek, and A. Zee, *Phys. Rev. B* **39**, 11413 (1989).
 - [3] H. Kawamura, *Phys. Rev. Lett.* **68**, 3785 (1992).
 - [4] N. D. Mermin and H. Wagner, *Phys. Rev. Lett.* **17**, 1133 (1966).
 - [5] A. Kolezhuk and T. Vekua, *Phys. Rev. B* **72**, 094424 (2005).
 - [6] J. Villain, *Ann. Isr. Phys. Soc.* **2**, 565 (1978).
 - [7] M. Affronte *et al.*, *Phys. Rev. B* **59**, 6282 (1999).
 - [8] S. V. Maleyev *et al.*, *J. Phys. Condens. Matter* **10**, 951 (1998); S. V. Maleyev, *Phys. Rev. Lett.* **75**, 4682 (1995).
 - [9] A. A. Nersisyan, A. O. Gogolin, and F. H. L. Essler, *Phys. Rev. Lett.* **81**, 910 (1998).
 - [10] M. Kaburagi, H. Kawamura, and T. Hikihara, *J. Phys. Soc. Jpn.* **68**, 3185 (1999); T. Hikihara *et al.*, *J. Phys. Soc. Jpn.* **69**, 259 (2000); Y. Nishiyama, *Eur. Phys. J. B* **17**, 295 (2000).
 - [11] I. P. McCulloch *et al.*, *Phys. Rev. B* **77**, 094404 (2008).
 - [12] K. Okunishi, *J. Phys. Soc. Jpn.* **77**, 114004 (2008).
 - [13] S. R. White, *Phys. Rev. Lett.* **69**, 2863 (1992); *Phys. Rev. B* **48**, 10345 (1993); K. Hallberg, *Adv. Phys.* **55**, 477 (2006); U. Schollwöck, *Rev. Mod. Phys.* **77**, 259 (2005); A.F. Albuquerque *et al.*, *J. Mag. Mat.* **310**, 1187 (2006).
 - [14] In the finite-system step, we keep up to $M = 1200$ states and perform up to 20 sweeps. The weight of the discarded states is of order 10^{-11} or smaller.
 - [15] A. A. Aligia, C. D. Batista, and F. H. L. Essler, *Phys. Rev. B* **62**, 3259 (2000).